pH-Responsive Microneedle Actuator Array For Precise Wound Healing: Design, Actuation, Light Filtering, and Evaluation

Mahsa Rastegar Pour
Department of Electrical Engineering
University of North Texas
Denton, TX 76207, USA
MahsaRastegarpour@my.unt.edu

Jun Ying Tan
Department of Electrical Engineering
University of North Texas
Denton, TX 76207, USA
JunYingTan@my.unt.edu

Rana Saha
Department of Medical Engineering
University of South Florida
Tampa, FL 33620, USA
ranasaha@usf.edu

Albert Kim
Department of Medical Engineering
University of South Florida
Tampa, FL 33620, USA
akim1@usf.edu

Jungkwun Kim
Department of Electrical Engineering
University of North Texas
Denton, TX 76207, USA
Jungkwun.Kim@unt.edu

2024 IEEE 17th Dallas Circuits and Systems Conference (DCAS) | 979-8-3503-4953-5/24/$31.00 ©2024 IEEE | DOI: 10.1109/DCAS61159.2024.10539863

Abstract—This paper presents a novel approach for wound healing utilizing an individually actuated microneedle array. The proposed system is designed to position each microneedle within distinct skin layers accurately. These microneedles are integrated into a housing supported by both hydrogel and gelatin layers, allowing precise microneedle control within various skin depths. A wound healing patch is a complex process influenced by localized pH variations. To address this, the system adapts microneedle placement based on the specific pH conditions of the wound site. The pH-sensitive nature of the dual-layer gel system enables expansion and contraction, facilitating deeper microneedle insertion under alkaline conditions typical of inner skin layers such as the dermis area and retracting microneedles closer to the surface (epidermis area) under acidic conditions near the skin's surface. This dual-layer actuation mechanism ensures not only sufficient force during microneedle insertion but also precise control throughout the wound-healing process. Controlled natural light will be irradiated through the microneedles and filtered ambient light by hydrogel in different pHs to efficient wavelengths. The paper includes an evaluation of key features such as actuation height, force application, and successful insertion tests conducted on pig skin, offering valuable insights into the system's performance.

Keywords—wound healing patch, microneedle array, dual-layer actuation, pH condition, force application, light filtering.

I. Introduction

In the sphere of medicine, a wound is defined as any difference or damage from the typical anatomical integrity and operational capacity of living tissue [1]. This encompasses a spectrum of injuries ranging from superficial abrasions to deep lacerations, each necessitating specific assessment and management strategies tailored to promote effective healing and tissue restoration [2]. Every year, approximately 20 million individuals worldwide grapple with chronic wounds, imposing a staggering financial burden of around USD 28 to 96 billion on healthcare systems. Despite the remarkable natural renewing abilities of human skin to heal damages and wounds, chronic wounds present persistent challenges that demand innovative solutions [3]. Wound healing is a complex biological process within the human body, comprising four essential phases: hemostasis, inflammation, proliferation, and remodeling [1]. When these phases proceed harmoniously, natural wound healing occurs. However, various factors, such as diabetes, age, hormonal imbalances, and other medical conditions, can significantly impact the effectiveness of the wound-healing process [1], [4]. pH, a significant physiological parameter, holds promise as a diagnostic tool for assessing physiological conditions. Its potential is particularly noteworthy in the evaluation of skin structure and wound status. Healthy skin is typically mildly acidic, with pH ranging from 4.1 to 5.8 [5], [6], and acts as a protective barrier against bacteria. However, the wounded skin layer typically exhibits an alkaline microenvironment, with pH ranging from 7.4 to 8.9 in chronic wounds, which fosters the growth of bacteria [7], [8]. Researchers have dedicated considerable effort to investigating novel smart wound dressings that incorporate pH sensors or controlled drug-release mechanisms, demonstrating innovative approaches to wound care [9]. In this paper, we engineered a gel-based dual-layer wound healing patch that leverages pH changes within wounds to autonomously adjust the light-guiding microneedle's position and the light-filtering hydrogel based on the dynamic response to the wound conditions, as depicted in Fig. 1. In fresh, alkaline, and humid wounds, the actuator expands, facilitating deeper penetration of microneedles. On the other hand, in partially and fully healed, acidic, and dry wounds, the actuator contracts, ensuring precise positioning. This dynamic adaptability is made possible through

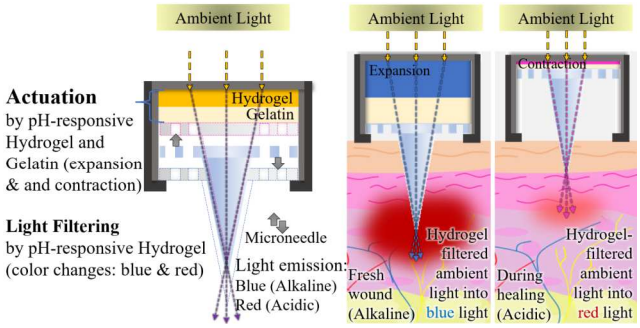

Fig.1. Conceptual drawing of wound healing on the wounded skin.

979-8-3503-4953-5/24/$31.00 ©2024 IEEE

the integration of a pH-sensitive hydrogel [10] and moisture-responsive gelatin, enabling accurate positioning of the microneedle within the wound. The pH-sensitive hydrogel also incorporates a light filtering feature to enable wound healing effects based on the wound's pH at various phases. In the fresh wound phase, where bacteria were facilitated to growth due to the alkaline microenvironment, the hydrogel filters blue-to-UV light into the wound for an antibacterial effect [11], whereas in the healed wound phase, the wound exhibits acidic microenvironment, the hydrogel filters red- light into the healed wound for skin cells and tissue proliferation [12]. The combination of the precise positioning of the light-guiding microneedle and the self-adjustable light filtering features presents itself as an advanced wound healing technique.

II. Method and Fabrication

The proposed design of the innovative wound healing patch includes five fundamental components, precisely integrated to achieve unique efficacy, and consist of an actuator housing, pH-sensitive hydrogel, humidity-sensitive gelatin, light-guiding microneedle, and a housing cap, as shown in Fig. 2. Fig. 2(a) illustrates the actuator housing, which was designed to have a size of 2.1 mm (L) × 2.1 mm (W) × 1 mm (H) to accommodate the hydrogel, gelatin, and the microneedle. The actuator housing and cap were 3D printed with a clear resin (FLGPCL04, Formlabs Inc.) using a stereolithography (SLA)-based 3D printer (Form 3, Formlabs Inc.) with a standard layer resolution of 50 µm. The pH-sensitive hydrogel casting solution was prepared as described in our prior work [10] and then dyed with a pH reagent for light filtering. 5 µL of the solution was drop-casted in the actuator housing, submerged in pH 7 buffer solution for 1 hr, then dried with compressed air, resulting in a final thickness of 200 µm, as shown in Fig. 2(b). For the humidity-sensitive gelatin layer, one part of gelatin powder and ten parts of deionized (DI) water were mixed using a magnetic

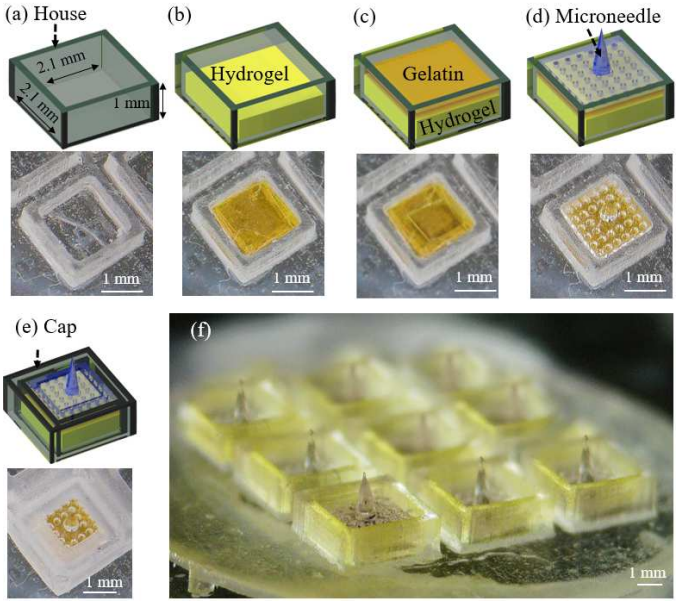

Fig. 2. Assembly of the wound healing patch, (a) Single cell of the house, (b) Single cell + hydrogel, (c) House + hydrogel + gelatin, (d) House + hydrogel + gelatin + microneedle, (e) House + hydrogel + gelatin + microneedle + cap, (f) Overview of the fabricated wound healing patch.

stirrer while heated to 180 °C for 5 min or until a homogeneous solution was obtained. Bubbles were carefully removed from the surface of the solution using a silicone spatula during the mixing process. 5 g of the bubble-free gelatin solution was uniformly cast on a pre-cleaned 25 mm × 25 mm glass substrate and allowed to dry naturally at room temperature to obtain a 200-µm thin gelatin film. The film was precisely machined to a 2 mm × 2 mm using a precision cutter and placed on top of the hydrogel layer inside the actuator housing, as shown in Fig. 2(c). The light-guiding microneedle, made of a biocompatible resin (FLSGAM01, Formlabs Inc.), was fabricated using a fabrication process known as diffraction lithography [13], [14], as shown in Fig. 2(d). The microneedle was fabricated to have a diameter of 500 µm and a height of 1500 µm. Furthermore, a 250-µm thick flat substrate was fabricated using the same principle and integrated into the microneedle to ensure a uniform vertical actuation. An array of holes was introduced to the substrate to allow unobstructed flow of liquid to the hydrogel and gelatin layers to ensure actuation uniformity. Lastly, the 3D-printed cap was glued to the actuator housing to encapsulate the hydrogel, gelatin, and microneedle inside the actuator housing, completing the wound healing patch while leaving an actuatable distance of 350 µm, as shown in Fig. 2(e). Fig. 2(f) demonstrates a prototype of the proposed wound healing patch in a 3×3 configuration, where the device size was 15 mm × 15 mm × 1.5 mm.

III. Result and Discussion

The actuator (hydrogel and gelatin layers) was first characterized for free-load actuation under various conditions. A single wound-healing unit was prepared for the testing, as shown in Fig. 3(a). To simulate the fresh wound environment, which typically exhibits an alkaline environment, a concentration of 2.73 µL/mm^3 of pH 10 environment was created by applying 10 µL of pH 10 solution to the cell and allowing it to actuate without load. Fig. 3(b) shows the result of the actuation 30 min after applying the pH 10 solution. An expansion of 350 µm from the baseline was measured, reaching the maximum expansion capacity of the cell. The alkaline and high humidity-driven expansion of the hydrogel and gelatin layers autonomously propels the microneedles deeper into wounds, allowing filtered incident light to be guided into deeper skin layers. In the condition of a wound healing state, which typically exhibits an acidic environment, a concentration of 2.73 µL/mm^3 of pH 4 environment was created to the cell using the same method and allowed for free-load actuation. Fig. 3(c) shows the results of the actuation 30 min after applying the pH

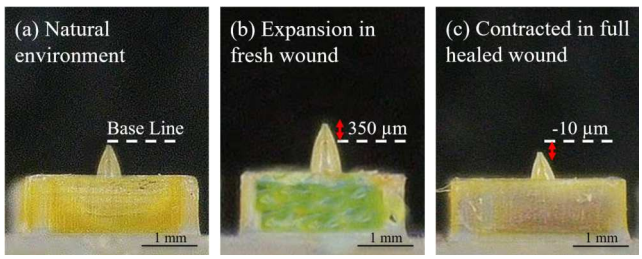

Fig. 3. Free-load actuation of single cell of wound patch in different pH solution, (a) pH 7, Natural environment, (b) pH 10, fresh wound, alkaline,

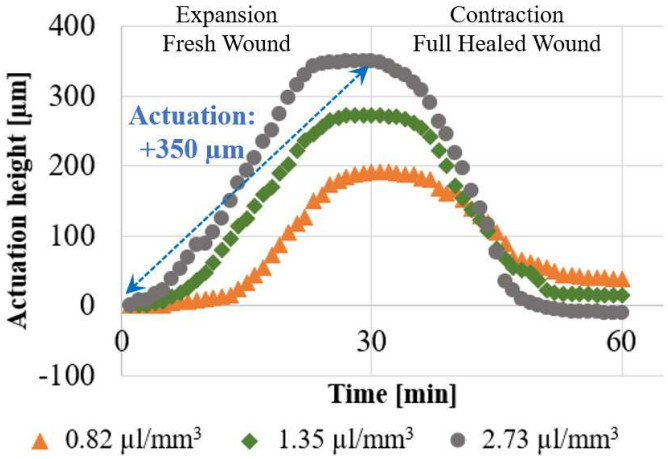

Fig. 4. Change of actuator's heights in response to different volume of pH solutions (pH 4, 7, and 10).

4 solution, reaching a –10 µm from the baseline due to the contraction of hydrogel in an acidic environment. The pH-sensitive contraction allows the microneedle to slowly withdraw from the deeper wound layers and eventually extract itself from the healed wound. Fig. 4 demonstrates an in-depth analysis of the actuation process with various concentrations of the pH environment. The actuation of the wound healing cell was examined in three different pH concentrations of 0.82, 1.35, and 2.73 µL/mm^3, each subject was allowed 30 min for free-load expansion, followed by 30 min of free-load contraction. The heights of the actuator were recorded every 1 min interval for the entire 60 min procedure. As a result, the pH concentration not only contributes to extensive actuation but also the rate of actuation. Fig. 4 shows that the actuator with pH concentration of 2.73 µL/mm^3 began to expand almost immediately after applying the pH 10 solution and rapidly reached to the maximum expansion of 350 µm in 23 min, whereas actuator with a lower pH concentration of 0.82 µL/mm^3 began to expand 13 min after applying the pH 10 solution and expanded to 190 µm at 30 min. Similar behavior has been observed in the contraction process as well. Note that the delay of expansion and contraction that occurred in the lower pH concentration schemes was due to the slower diffusion rate of pH solution into the pH-sensitive hydrogel.

Subsequently, the force generated during the expansion and contraction of the actuator was subjected to a force test to

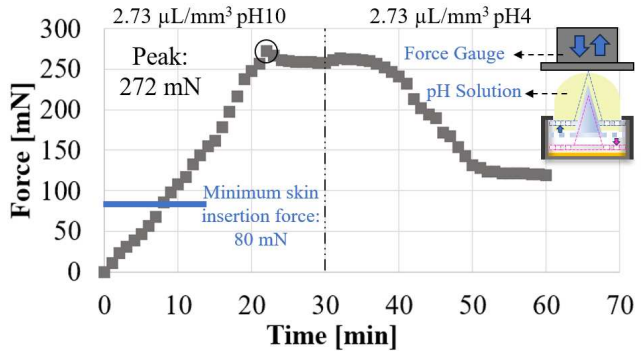

Fig. 5. Force test results with 2.73 µL/mm^3 pH 10 and 4 solutions.

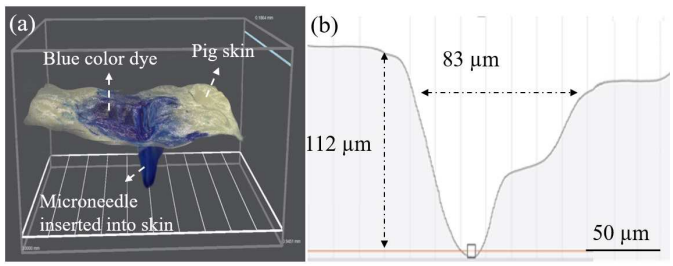

Fig. 6. Pig skin insertion test result, (a) 3D topology after insertion test, (b) Cross-sectional measurement of the insertion.

validate the practicality of the actuator in a wound application as shown in Fig. 5. A single wound healing cell was mounted under a stationary force gauge, while only the microneedle tip was contacting with the force gauge. A concentration of 2.73 µL/mm^3 pH 10 environment was applied to the cell and allowed for expansion for 30 min, followed by pH 4 environment with the same concentration for 30 min. A constant increment in force was measured until a peak force of 272 mN has reached at the 22nd min and remained constant until pH 4 was applied at 30th min. The force remained constant until the 37th min where the contraction began as the hydrogel became acidic. The actuated force slowly reduced to 121 mN at the 51st min, where the contraction was completed. The minimum insertion force into skin for microneedle has been reported to be 80 mN [15], which is lower than the measured force throughout the actuation process, validating the practicality of the actuators in wound applications. To further verify the functionality of the microneedle, a skin insertion test was conducted. Fig. 6 shows the insertion result of a single wound healing microneedle device into a pig cadaver skin using mild thumb pressure. The 3D profile of the insertion site was captured using an automated digital microscope (Smartzoom 5, Zeiss) and the result is shown in Fig. 6(a). Fig. 6(b) shows the cross-sectional view of the insertion site, showing an insertion depth of 112 µm and a width of 83 µm, verifying the microneedle's functionality.

Lastly, the light filtering feature of the hydrogel layer was evaluated to validate the wound healing effects. A 3×3 wound healing patch was positioned 1 mm above a spectrometer, while filtering the ambient light incident at the back of the patch. Various pH conditions, including acidic, neutral, and alkaline were applied to the hydrogel and Fig. 7 shows the spectrum of the filtered light captured by the spectrometer. The hydrogel filters the broadband ambient light into nm, simulating the scenario before applying it to a wound. When the patch was subjected to an alkaline environment, such as a fresh wound, the hydrogel filtered the wavelengths from 377 to 472 nm, primarily blue light, promoting the antibacterial effects. Conversely, when the patch was subjected to an acidic environment, such as a partially or fully healed wound, the hydrogel permits wavelengths from 604 to 684 nm, which are red light, allowing cells and tissue proliferation effects. This innovative light filtering feature promotes optimal and targeted wound healing effects, especially fit to address the complex wound recovery requirements.

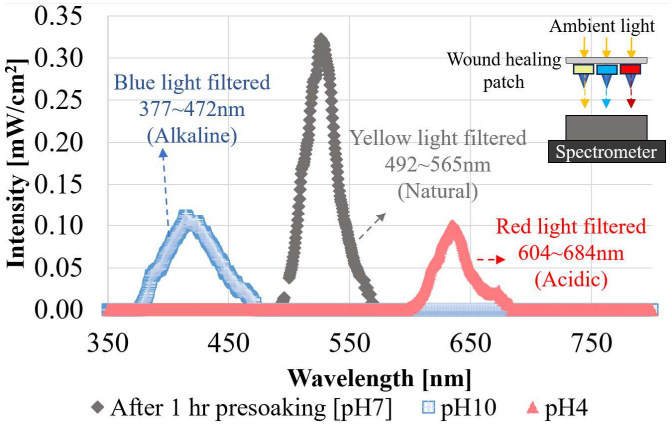

Fig. 7. Light filtering results in pH 7, 4, and 10 solutions.

IV. Conclusion

The design, fabrication and two key features (actuation and light filtering) of the proposed wound healing patch has been extensively discussed in the paper. The pH-sensitive hydrogel layer was demonstrated with remarkable versatility in response to alkaline and acidic environments, realizing the automatic self-positioning feature of the microneedle within the wound as well as the light filtering function for various wound healing effects. The humidity-sensitive gelatin layer served as a supportive element, which supplied sufficient force to the microneedle for deep skin penetration. The light-guiding microneedle was integrated to the device that focused the dim, filtered ambient light to the tip to deliver a sufficient light intensity to the desired target. A series of experiments were conducted, including actuation based on the concentration of the pH solution, actuation force, skin insertion test, and light filtering test to attest the efficacy of the proposed wound healing patch for advance wound applications. The results underscore its innovative design and dynamic responsiveness to varying pH environments, as similarly expressed in wound healing process. This multifaceted approach holds great potential for addressing the involved challenges associated with wounds, paving the way for a new era in advanced wound healing technologies.

Acknowledgment

The research was supported by the National Science Foundation (NSF) CNS 2039014, ECCS 2326938, ECCS 2325032, ECCS 2029077, and Korea Evaluation Institute of Industrial Technology (KEIT) 20018023.

References

[1] S. Guo and L. A. DiPietro, "Factors Affecting Wound Healing," *J. Dent. Res.*, vol. 89, no. 3, pp. 219–229, Mar. 2010, doi: 10.1177/0022034509359125.

[2] B. K. Sun, Z. Siprashvili, and P. A. Khavari, "Advances in skin grafting and treatment of cutaneous wounds," *Science*, vol. 346, no. 6212, pp. 941–945, Nov. 2014, doi: 10.1126/science.1253836.

[3] C. K. Sen, "Human Wound and Its Burden: Updated 2020 Compendium of Estimates," *Adv. Wound Care*, vol. 10, no. 5, pp. 281–292, May 2021, doi: 10.1089/wound.2021.0026.

[4] S. C. Gilliver, J. J. Ashworth, and G. S. Ashcroft, "The hormonal regulation of cutaneous wound healing," *Clin. Dermatol.*, vol. 25, no. 1, pp. 56–62, Jan. 2007, doi: 10.1016/j.clindermatol.2006.09.012.

[5] E. Proksch, "pH in nature, humans and skin," *J. Dermatol.*, vol. 45, no. 9, pp. 1044–1052, Sep. 2018, doi: 10.1111/1346-8138.14489.

[6] H. Lambers, S. Piessens, A. Bloem, H. Pronk, and P. Finkel, "Natural skin surface pH is on average below 5, which is beneficial for its resident flora," *Int. J. Cosmet. Sci.*, vol. 28, no. 5, pp. 359–370, Oct. 2006, doi: 10.1111/j.1467-2494.2006.00344.x.

[7] G. Power, Z. Moore, and T. O'Connor, "Measurement of pH, exudate composition and temperature in wound healing: a systematic review," *J. Wound Care*, vol. 26, no. 7, pp. 381–397, Jul. 2017, doi: 10.12968/jowc.2017.26.7.381.

[8] L. A. Schneider, A. Korber, S. Grabbe, and J. Dissemond, "Influence of pH on wound-healing: a new perspective for wound-therapy?," *Arch. Dermatol. Res.*, vol. 298, no. 9, pp. 413–420, Feb. 2007, doi: 10.1007/s00403-006-0713-x.

[9] S.-H. Kuo, C.-J. Shen, C.-F. Shen, and C.-M. Cheng, "Role of pH Value in Clinically Relevant Diagnosis," *Diagnostics*, vol. 10, no. 2, p. 107, Feb. 2020, doi: 10.3390/diagnostics10020107.

[10] R. Campbell, J. Y. Tan, A. Santiago, J. Kim, and A. Kim, "Hydrogel Actuated Microneedle (HAM) Wound Patch," *Hilton Head Workshop 2022 Solid-State Sens. Actuators Microsyst. Workshop*, Jun. 2022.

[11] R. Yin *et al.*, "Light based anti-infectives: ultraviolet C irradiation, photodynamic therapy, blue light, and beyond," *Curr. Opin. Pharmacol.*, vol. 13, no. 5, pp. 731–762, Oct. 2013, doi: 10.1016/j.coph.2013.08.009.

[12] A. Gupta, T. Dai, and M. R. Hamblin, "Effect of red and near-infrared wavelengths on low-level laser (light) therapy-induced healing of partial-thickness dermal abrasion in mice," *Lasers Med. Sci.*, vol. 29, no. 1, pp. 257–265, Jan. 2014, doi: 10.1007/s10103-013-1319-0.

[13] J. Y. Tan *et al.*, "Experimental Validation of Diffraction Lithography for Fabrication of Solid Microneedles," *Multidiscip. Digit. Publ. Inst. Mater.*, vol. 15, no. 24, p. 8934, 2022.

[14] S. F. Shiba, J. Y. Tan, and J. Kim, "Multidirectional UV-LED lithography using an array of high-intensity UV-LEDs and tilt-rotational sample holder for 3-D microfabrication," *Micro Nano Syst. Lett.*, vol. 8, no. 1, p. 5, Apr. 2020, doi: 10.1186/s40486-020-00107-y.

[15] S. P. Davis, B. J. Landis, Z. H. Adams, M. G. Allen, and M. R. Prausnitz, "Insertion of microneedles into skin: measurement and prediction of insertion force and needle fracture force," *J. Biomech.*, vol. 37, no. 8, pp. 1155–1163, Aug. 2004, doi: 10.1016/j.jbiomech.2003.12.010.